

A Comparative Study on Corrosion Behavior of Ti-35Nb-5Ta-7Zr, Ti-6Al-4V and CP-Ti in 0.9 wt% NaCl

Viswanathan S. Saji, Yong Hoon Jeong, and Han Cheol Choe[†]

Department of Dental Materials, School of Dentistry, Chosun University, Gwangju 501-759

(Received June 1, 2009; Revised July 18, 2009; Accepted July 19, 2009)

Recently, quaternary titanium alloys of the system Ti-Nb-Ta-Zr received considerable research interest as potential implant materials because of their excellent mechanical properties and biocompatibility. However, only few reported works were available on the corrosion behavior of such alloys. Hence, in the present work, electrochemical corrosion of Ti-35Nb-5Ta-7Zr alloy, which has been fabricated by arc melting and heat treatment, was studied in 0.9 wt% NaCl at 37 ± 1 °C, along with biomedical grade Ti-6Al-4V and CP-Ti. The phase and microstructure of the alloys were investigated employing XRD and SEM. The results of electrochemical studies indicated that the corrosion resistance of the quaternary alloy was inferior to that of Ti-6Al-4V and CP Ti.

Keywords : Ti-35Nb-5Ta-7Zr, biomaterial, corrosion

1. Introduction

Titanium alloys of the system Ti-Nb-Ta-Zr are receiving more attention as orthopedic and dental implant materials because of their excellent mechanical properties such as very low elastic modulus coupled with superior biocompatibility.¹⁻⁵⁾ The aim of developing low modulus titanium alloys was to decrease the elastic modulus difference between the natural bone (10-30 GPa) and the implant material, thereby promoting load sharing between them.⁶⁾ Major quaternary alloys of Ti-Nb-Ta-Zr system investigated include Ti-4Nb-4Ta-15Zr,²⁾ Ti-29Nb-13Ta-4.6Zr¹⁾ and Ti-35Nb-5Ta-7Zr.³⁾ Among these, Ti-35Nb-5Ta-7Zr has a lower elastic modulus of 55 GPa and can be considered as one of the potential candidate for implant applications.^{3),7)}

However, reported information available on electrochemical corrosion behavior of Ti-Nb-Ta-Zr based alloys is limited.^{2),5),8),9)} Ti-15Zr-4Nb-4Ta alloy has been developed by Okazaki who also evaluated its corrosion resistance and fatigue properties.²⁾ Impedance spectroscopy studies of Ti-29Nb-13Ta-4.6Zr alloy in Hank's solution suggested formation of a bi layer passive film with an outer porous layer on the surface.^{5),8)} Kim et al has compared the corrosion resistance of two high Ta containing Ti-Nb-Ta-Zr alloys.⁹⁾ In this context, we have investigated

electrochemical corrosion behavior of Ti-35Nb-5Ta-7Zr (TNTZ) alloy in 0.9 wt% NaCl at 37 ± 1 °C. The results were compared with biomedical grade Ti-6Al-4V (TAV) alloy and CP Ti, under similar experimental conditions.

2. Methodology

The TNTZ alloy was fabricated by arc melting with non consumable tungsten electrode and water cooled copper hearth under ultra pure argon atmosphere. Commercially high pure Ti, Nb, Ta and Zr were employed for the purpose. All the ingots were melted and inverted 10 times in order to homogenize the alloy chemical composition. To stabilize the β phase and to homogenize the microstructure, the casted alloy was heat treated at 1000 °C for 2 h in Ar atmosphere, followed by water quenching. The homogenized alloy was sectioned, mounted using epoxy, polished by silicon carbide papers of different grades from 100 to 2000 and finally alumina polished. The arc melted TAV alloy was heat treated at 1000 °C for 12 h and water quenched. The heat treatment carried out for CP-Ti was 1000 °C for 24 h, followed by water quenching.

The chemical composition and phase of the alloys were identified by energy dispersive X-ray spectroscopy (EDS, JXA-8900M, Jeol, Japan) and X-ray diffraction, using a Cu- α radiation (XRD, X'pert Pro, Philips, Netherlands), respectively. Chemical etching was performed using Keller's reagent (HF+HCl+HNO₃+H₂O) and the microstructure

[†] Corresponding author: hcchoe@chosun.ac.kr

was observed by scanning electron microscope (FE-SEM Hitachi 4800, Japan). The chemical composition of the quaternary and ternary alloy as determined by EDS was Ti: Nb: Ta: Zr = 51.6: 35.5: 5.1: 7.8. and Ti: Al: V = 89.2: 6.5: 4.3.

Potentiodynamic anodic polarization experiments were carried out employing a EG&G, 263A potentiostat/ galvanostat. A conventional three electrode system with high density graphite as counter electrode and saturated calomel electrode (SCE) as reference was used. The sample was mounted in a cold mount epoxy resin. The sample edges were carefully covered with epoxy to avoid the possible crevice attack. The electrolyte used was 0.9 wt% NaCl at 37 ± 1 °C. Analytical reagent grade chemical and double de-ionized water was used. The electrolyte was de-aerated with high purity Ar gas for 30 min before starting the experiment. De-aeration was continued at a uniform rate during the experiment and the solution was subjected to mild stirring using a magnetic stirrer. The scan rate used was 1.667 mV/s.

Electrochemical impedance spectroscopy studies were carried out using a similar three electrode set-up, employing EG&G 1025 impedance analyzer and controlled by powersuite software. The frequency range used for EIS studies was 10^{-1} Hz to 10^5 Hz. The amplitude of AC signal was 10 mV and 5 points per decade was used.

3. Results and discussion

3.1 Phase and microstructure

The microstructure of TNTZ, TAV and CP-Ti are shown in Fig. 1(a-c), respectively. The micrographs of as-etched TNTZ alloy revealed equiaxed β grains. The CP-Ti exhibited typical rapidly cooled metastable feather like microstructure that consists of equiaxed α grain with some twin bands. The microstructure of Ti-6Al-4V alloy revealed $\alpha + \beta$ structure consists of elongated α grains and intergranular β grains. In Ti-6Al-4V, the 6 wt% Al stabilizes the α phase and 4 wt% V stabilizes the beta phase. The comparatively higher elastic modulus of the Ti-6Al-4V is attributed to the higher volume fraction of the alpha phase. In the case of the TNTZ alloy, the alloying elements Nb and Ta are strong β stabilizers.

The X-ray diffraction pattern of TNTZ, TAV and CP-Ti are shown in Fig. 2. The XRD pattern of CP-Ti is comprised entirely of hexagonal α phases; whereas the Ti-6Al-4V alloy exhibits the presence of both α and β phases. The XRD spectra of TNTZ alloy revealed distinct peaks of body centered cubic, (110), (200), (211) and (220); corresponding to the single β phase. From the phase diagram¹⁰⁾ and the heat treatment followed in this study, it

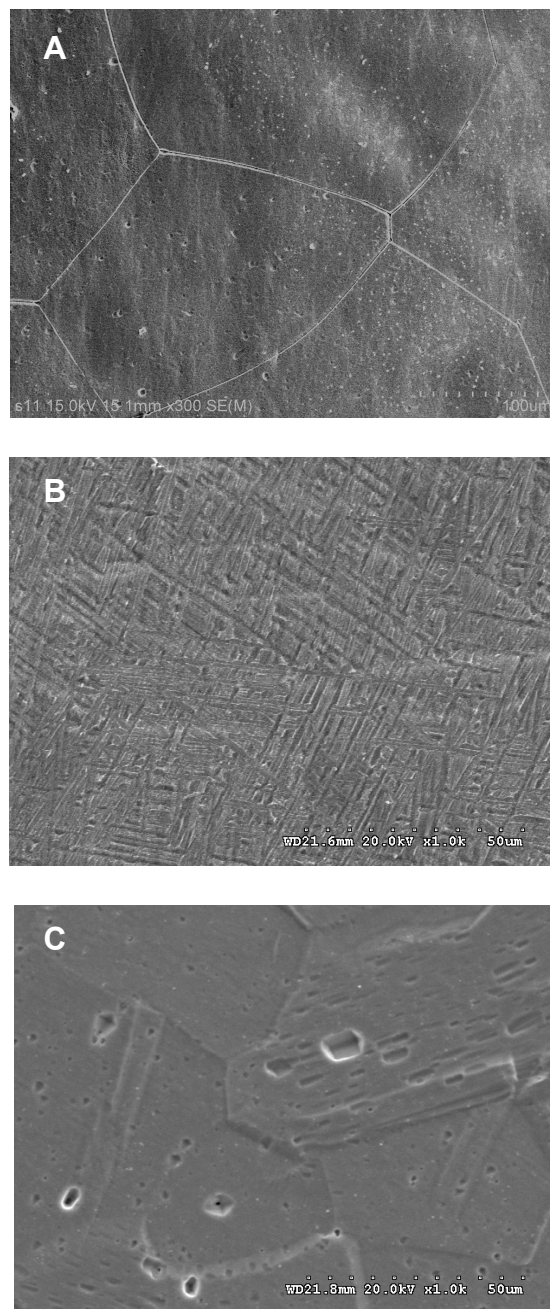


Fig. 1. Representative SEM micrographs of (A) TNTZ (B) TAV (C) CP-Ti

can be inferred that the metastable β phase was retained completely in the TNTZ alloy.

3.2 Electrochemical studies

Fig. 3 shows the potentiodynamic anodic polarization plots recorded for the TNTZ, TAV and CP Ti. An immersion period of 1 h was given for stabilization of open circuit potential (OCP) before starting the experiment. A stable passive region was formed in the case of TNTZ

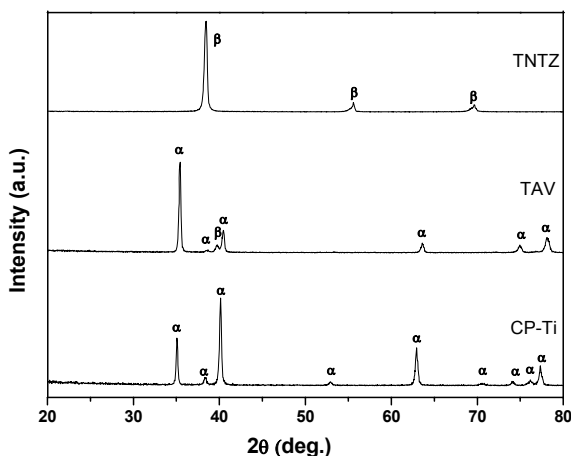


Fig. 2. Representative XRD pattern of (A) TNTZ (B) TAV (C) CP-Ti

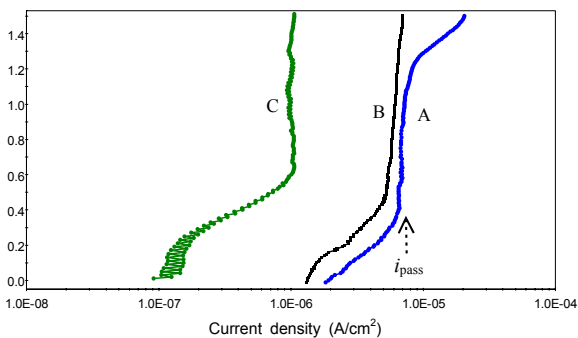


Fig. 3. Potentiodynamic anodic polarization plots of (A) TNTZ (B) TAV (C) CP-Ti.

alloy at an applied potential of ~ 0.35 V (E_{pass}). This passive region was characterized by a passive current density (i_{pass}) of the order of 10^{-6} A/cm². The corresponding E_{pass} of TAV and CP Ti was ~ 0.45 and ~ 0.58 V respectively. Such a trend probably indicates that the quaternary alloy reached the passivation region at a lower applied potential. However, the i_{pass} decreased in the order TNTZ > TAV > CP-Ti. An increase in current density was observed for the TNTZ alloy when polarized above 1.5 V. This may be associated with a possible passive film breakdown. The ternary alloy and CP-Ti showed more extended potential range of passive film stability. The much spikes observed at lower potentials for CP-Ti may be associated with the lower current level of the order of 10^{-7} A/cm².

After the potentiodynamic polarization experiment, the quaternary alloy surface was examined to identify the sites of corrosion attack, if any. There were few locally attacked areas when the sample was polarized above 2 V. An EDS line analysis (Fig. 4) was followed across a locally attacked area. As expected, severe depletion of Ti occurred

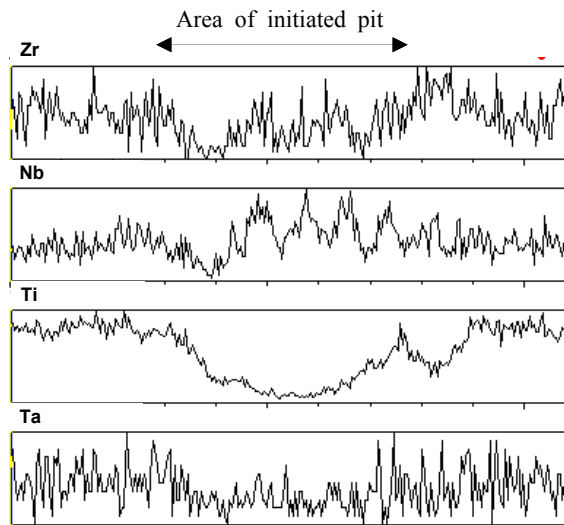


Fig. 4. EDS line scan analysis across a locally attacked area, above the breakdown potential.

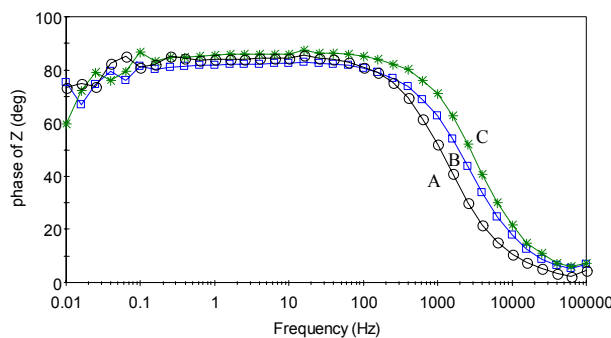
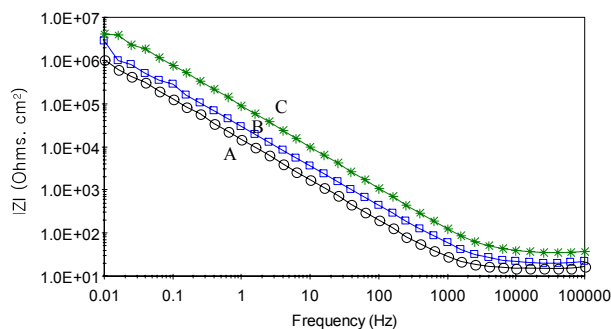


Fig. 5. Bode spectra recorded at E_{corr} of (A) TNTZ (B) TAV (C) CP-Ti

at the attacked area due to the local destruction of titanium oxide based passivation; the main cause of passive film breakdown. The average composition (in wt%) of a selected area of the corroded surface as quantified by EDS was Ti: Nb: Ta: Zr = 34.92: 24.76: 25.54: 14.78. The least tantalum dissolution from the corroded area may be associated with the relatively more resistance of Ta₂O₅ to chlorine attack.¹¹⁾

Table 1. EIS simulation result

Alloy	TNTZ		TAV		CP-Ti	
	E_{corr}	0.3 V	E_{corr}	0.3 V	E_{corr}	0.3 V
$R_p / \text{M}\Omega \cdot \text{cm}^2$	4.64	5.74	8.19	9.40	10.14	11.26
$C / \mu\text{F} \cdot \text{cm}^{-2}$	12.52	10.59	6.17	5.80	2.25	1.98
n	0.94	0.94	0.92	0.92	0.94	0.94

The non-destructive EIS plots supported the polarization results. Fig. 5 represents the impedance Bode spectra recorded at E_{corr} for TNTZ, TAV and CP-Ti. A period of 30 min was given for stabilization of OCP before starting the experiment. The similar impedance behavior of the quaternary, ternary and CP-Ti indicates a similar nature of passivation as TiO_2 based passivation is controlling the interface. The phase shift plots exhibited pure capacitive behavior with one time constant indicating single and compact passive film formation at the interface. A simple Randles equivalent circuit model consisting of a constant phase element (CPE) which represents oxide film capacitance in parallel with oxide film resistor (R_p); both in series with the solution resistance (R_s) can be used to describe the experimental results. Chi-square values of the order of 10^{-3} indicated excellent agreement between the experimental and model values and the simulated values obtained are shown in Table 1. A higher value of R_p implies higher corrosion resistance. The n values close to 1 show near capacitive behavior.

Hence the results of the present study indicated that the corrosion resistances of the alloys were in the increasing order TNTZ < TAV < CP-Ti. It is expected that the TNTZ alloy should have a higher corrosion resistance than the TAV alloy; due to the formation of the protective oxide film composed of oxides of Ti, Nb, Ta and Zr (TiO_2 , Nb_2O_5 , Ta_2O_5 and ZrO_2) on metal surface. However it should be noted that the heat treatment conditions followed for the three alloys was different. Rather than the differ-

ence in the alloy phase, the lower corrosion resistance obtained for the TNTZ alloy may be associated with the alloy composition as well as the heat treatment followed.

4. Conclusions

The microstructure and structural characteristics confirm that Ti-35Nb-5Ta-7Zr alloy possess equiaxed β phase in its microstructure. Results of electrochemical corrosion studies suggested that the corrosion resistance of the alloys were in the increasing order Ti-35Nb-5Ta-7Zr < Ti-6Al-4V < CP Ti.

References

1. M. Niinomi, T. Akahorin, K. Morikawa, T. Kasuga, A. Suzuki, H. Fukui, and S. Niwa, *Mater. Trans.*, **43**, 2970 (2002).
2. Y. Okazaki. *Curr. Opin. Solid State Mater. Sci.*, **5**, 45 (2001).
3. E. B. Taddei, V. A. R. Henriques, C. R. M. Silva, and C. A. A. Cairo, *Mater. Sci. Eng.*, **C 24**, 683 (2004).
4. J. I. Qazi, B. Marquardt and H. J. Rack, *JOM- J. Min. Met. Mater. Soc.*, **56**, 49 (2004).
5. M. Karthega, V. Raman and N. Rajendran, *Acta Biomater.*, **3**, 1019 (2007).
6. M. Long, and H. J. Rack, *Biomaterials*, **19**, 1621 (1998).
7. *ASTM Designation Draft #3*, "Standard Specification for Wrought Ti-35Ni-7Zr-5Ta Alloy for Surgical Implant Applications (UNS R58350)", ASTM, Philadelphia, PA, 2000.
8. V. Raman, S. Nagarajan and N. Rajendran, *Electrochem. Commun.*, **8**, 1309 (2006).
9. S. E. Kim, J. H. Son, Y. T. Hyun, H. W. Jeong, Y. T. Lee, J. S. Song and J. H. Lee, *Met. Mater. Inter.*, **13**, 151 (2007).
10. X. Tang, T. Ahmed and R. J. Rack, *J. Mater. Sci.*, **35**, 1805 (2000).
11. *ASM International Handbook*, Corrosion, Vol. 13, ASM International, 1987.